Disclaimer

This note has not been internally reviewed by the DØ Collaboration. Results or plots contained in this note were only intended for internal documentation by the authors of the note and they are not approved as scientific results by either the authors or the DØ Collaboration. All approved scientific results of the DØ Collaboration have been published as internally reviewed Conference Notes or in peer reviewed journals.

A Test of QCD Based on
the Topologies of the Three- and Four-Jet Events

Jianming Qian

Department of Physics

The University of Michigan, Ann Arbor, Michigan 48109

Abstract

The global topologies of the three- and four-jet events produced in the $\bar{p}p$ interaction are described. The three- and four-jet events are selected from data recorded by the DØ detector at the Tevatron collider operating at a center-of-mass energy of $\sqrt{s} = 1800$ GeV. The distributions of various topological variables are compared with the leading order QCD calculations and with the predictions of PYTHIA and HERWIG parton shower models. The leading order QCD calculations are found to be in good agreement with the data, while the PYTHIA and HERWIG models provide a less satisfactory description of the structures of the three- and four-jet events.

Introduction

The Fermilab Tevatron collider provides an unique opportunity to study the properties of hard interactions in $\bar{p}p$ collisions at short distances. The hard scattering is described by the theory of perturbative Quantum ChromoDynamics (QCD) [1, 2, 3] and has been studied extensively in the last decade [4, 5]. Within the content of QCD, the hard process is described as the point-like scattering between constituent partons (quarks and gluons) of protons and anti-protons, convoluted with parton momentum distributions inside the nucleon. The cross sections for the scattering can be written in expansions of the strong coupling constant α_s. The lowest order $\mathcal{O}(\alpha_s^2)$ term corresponds to the production of two-parton final state. Terms of $\mathcal{O}(\alpha_s^3)$ and of $\mathcal{O}(\alpha_s^4)$ in the expansion imply the existence of the three- and four-parton final states. Coloured partons from hard scattering evolve soft quark and gluon radiation and the hadronization process to form detectable colorless hadrons, which appear in the detector as localized energy deposits identified as jets. Jets originating from partons in the initial hard scattering process are typically isolated from other collision products and have large transverse energies. They preserve the energy and direction of the initial partons. Therefore, the topologies of final jet system are directly related to those of initial parton system.

The cross section and angular distributions for two-jet events have been successfully compared with the predictions of QCD [5, 6]. A study of the three- and four-jet events allows one to test the validity of QCD to higher order (α_s^3 or beyond) and to probe the underlying QCD dynamics. This note explores the topological variables of the three- and four-jet events. The measured distributions of these variables are compared with the leading order QCD calculations as well as with the predictions of parton shower based Monte Carlo models. Topological distributions for the three- and four-jet events have been published previously by UA1, UA2 and CDF [7, 8, 9]. This note describes a more comprehensive study of the topological distributions of the three- and four-jet events with a higher statistics data sample. It also extends the study to phase space un-probed and to the models untested previously. The production cross sections and the p_T distributions of multi-jet final states are not the subject of this note. These will be discussed in a separate forth coming note.

Definition of Topological Variables

The topological variables of the three- and four-jet events investigated in this note are defined in this section. As far as the definitions are concerned, partons and jets are the same objects. For simplicity of description, the two terms are used interchangeably. The topological variables are defined in the parton or jet center-of-mass system (CMS).

Assuming massless partons, the topological properties of the three-parton final state in their center-of-mass system can be described in terms of six variables. Three of the variables define how the CMS energy is shared among the three final state partons. The other three variables define the orientation of the plane containing the three partons in space. It is convenient to introduce the notation: $1 + 2 \to 3 + 4 + 5$ for the three-parton process. Here number 1 and 2 refer to incoming partons while number 3, 4 and 5 label the outgoing partons, ordered in descending CMS energies, i.e. $E_3 > E_4 > E_5$. The final state parton energies are the obvious choices for the topological variables. For simplicity, $E_i (i = 3, 4, 5)$ are often replaced by the scaled variables $x_i (i = 3, 4, 5)$, which are defined by $x_i = \frac{2E_i}{\sqrt{\hat{s}}}$, where $\sqrt{\hat{s}}$ is the subprocess center-of-mass energy. By definition, $x_3 + x_4 + x_5 = 2$. Clearly only two of the scaled variables are relevant for topological studies. The angle variables can be chosen

2

to be: (1) the cosine [1] of polar angle $(\cos\theta^*)$ and (2) the azimuthal angle (ϕ^*) of parton 3, (3) the angle (ψ^*) between the plane containing parton 1 and 3 and the plane containing parton 4 and 5 defined by:

$$\cos\psi^* = \frac{\vec{p}_1 \times \vec{p}_3 \cdot \vec{p}_4 \times \vec{p}_5}{|\vec{p}_1 \times \vec{p}_3||\vec{p}_4 \times \vec{p}_5|},$$

where $\vec{p}_i (i = 1, ..., 5)$ is the parton momenta. For unpolarized beams (as they are at Tevatron), the ϕ^* distribution is uniform. Therefore, only four independent kinematic variables are needed to describe the topological properties of the three-parton final state and they are typically chosen to be x_3, x_4, $\cos\theta^*$ and ψ^*. Another variable of interests is the asymmetry between parton 4 and 5 defined as:

$$\cos\delta = \frac{E_4 - E_5}{E_3}$$

It can be shown that δ is the angle between parton 3 and 5 in the rest frame of parton 4 and 5. Historically, $\cos\delta$ distribution provided the first test of gluon spin at e^+e^- collider [10].

The situation with the four-parton final state is more complicated. Apart from the CMS energy, eight independent parameters are needed to completely define a four-parton system in their center-of-mass system, assuming partons are massless. Two of them define the overall event orientation while the other six fix the internal structure of the four-parton system. Similar to the three-parton final state, one of the two variables fixing the event orientation can be chosen to be the azimuthal angle of the leading parton, which is uniformly distributed for unpolarized beams. In contrast to the three-parton final state, the choices of topological variables are less obvious. There is a variety of space angle distributions. For example, in their recent publication, UA2 [8] and CDF [9] examined the angles of jet pairs in the center-of-mass system. In this note, two sets of variables are examined. One set of variables is those space angles studied by UA2 and CDF. To define these variables, the partons are ordered in decreasing order of p_T and labeled from 3 to 6. The space angles between jets in their center-of-mass system, $\cos\Omega_{ij}(i, j = 3, ..., 6)$, are sensitive probes of the structure of the four-parton final state. The definition of the second set variables follows closely with those used for the three-parton final state. Four partons are ordered in descending CMS energy and labeled from 3 to 6. This set of variables includes the scaled energies of the two non-leading partons (x_5 and x_6), the cosine ($\cos\theta^*$) of the leading jet polar angle and the angle (ψ^*) between the plane defined by the two leading partons and the plane defined by two non-leading partons.

The Theoretical Model

The cross section for the production of n-parton final state $1 + 2 \rightarrow 3 + ... + (n + 2)$ in $\bar{p}p$ collision at center-of-mass energy $\sqrt{s}$ is described by the following generic form:

$$\sigma_n = \sum_\ell \int f_1^\ell(x_1) f_2^\ell(x_2) |M_\ell^n|^2 \Phi_n dx_1 dx_2$$

where $\sum_\ell$ sums over all possible $1 + 2 \rightarrow n$-parton subprocesses. $f_1^\ell(x_1)$ and $f_2^\ell(x_2)$ are the parton density distribution of incoming partons. $|M_\ell^n|^2$ stands for the matrix elements for the subprocess and Φ_n is n-body phase space. In general, to the lowest order $|M_\ell^n|^2 \propto \alpha_s^n/\sqrt{s}$ with $\hat{s} = x_1 x_2 s$.

---

[1] Unless otherwise specified, the absolute values on the cosines are implied through out this note.

Theoretically $|M_f^n|^2$ is well behaved if calculated to all orders in the α_s expansion. Practically, such calculation is technically not possible. Therefore one has to deal with the truncated matrix element in the α_s expansion. As results, $|M_f^n|^2$ diverges when the energy of any final state parton or the angle between any two partons approaches zero, due to the bremsstrahlung nature of quark and gluon radiation. The singularities in $|M_f^n|^2$ cause poles in the topological distributions.

Two approaches in modeling perturbative QCD for multi-jet production exist. The straight forward method is the matrix element method, in which Feynman diagrams are calculated order by order in α_s. The technical difficulties have limited the calculations to the leading order of the concerned processes. The exact lowest order $\mathcal{O}(\alpha_s^3)$ matrix elements calculation for the three-parton final state has been available for some time [11]. The complete leading order matrix calculation for up to five-parton final state has also been available in the form of Berends-Giele-Kuijf (BGK) [12] program. The other commonly used approximate calculations are those of of Kunszt-Stirling (KS) [13] and of Maxwell [14]. The matrix element method generally describes hard and non-collinear gluon radiation and splitting better than the case of soft and collinear gluon radiation. The second approach is based on the parton shower scheme. In this method, the hard scattering begins with two initial partons, an arbitrary number of partons are then branched off from the initial partons to yield a description for multi-parton production, with no explicit upper limit on the number of partons involved. The parton shower picture is derived within the framework of Leading-Logarithmic Approximation (LLA) [15]. As a result of the approximation, the reliability of the parton shower decreases as parton multiplicity increases.

Different perturbative QCD approaches have been incorporated into several Monte Carlo programs. For the analysis described in this note, PAPAGENO [16], PYTHIA 5.6 [17], and HERWIG 5.6 [18] are chosen as examples. This set of Monte Carlo reflects different approaches of perturbative QCD and fragmentation models. PAPAGENO is a partonic event generator. It implements exact matrix element calculation for tree level contributions up to the three-parton final state and provides approximate calculations up to six-parton final state. Both HERWIG and PYTHIA are parton shower based Monte Carlo programs. Only two initial partons are produced at the hard scattering. Additional partons are branched off at parton shower phase. These two Monte Carlo programs differ in the implementation of QCD interference phenomena and the treatment of parton shower development. Another difference between these two programs is the fragmentation models used. PYTHIA uses QCD inspired string fragmentation [19] while HERWIG employs cluster fragmentation [20].

The Data Sample

The data used in this analysis was collected by the D∅ detector during the 1992-1993 Tevatron run at a center-of-mass energy of 1800 GeV. An integrated luminosity of 15.5 pb^{-1} was recorded in the run. With fine segmentation ($\Delta\eta \times \Delta\phi = 0.1 \times 0.1$) and the unprecedented rapidity coverage ($-4.5 < \eta < 4.5$) of the calorimeter, the D∅ detector is specially suited for studying multi-jet physics. The detailed description of the D∅ detector can be found elsewhere [21].

The events used in this study had to pass a hardware (Level-1) and a software (Level-2) cluster based triggers. The Level-1 trigger was based on the calorimeter energy deposited in towers of size $\Delta\eta \times \Delta\phi = 0.2 \times 0.2$. The events were required to have at least two such towers with registered transverse energy (p_T) above 7.0 GeV. The successful candidates were passed to the level-2 trigger, which sums transverse energies of calorimeter towers within a radius of $R(\equiv (\Delta\eta^2 + \Delta\phi^2)^{1/2}) = 0.7$. The level-2 trigger selects those events with at least one such cone, built around the level-1 trigger

tower, with transverse energy above 50.0 GeV. Taking into account the trigger pre-scale factor, the total effective luminosity is 1.2 pb^{-1}. The trigger efficiency for events with at least one jet with $p_T > 60$ GeV is above 90%. A detailed description of triggers can be found elsewhere [22].

The offline reconstruction uses a cone jet algorithm first used by UA1 [23] with R=0.7, similar to the algorithm used in the level-2 trigger. The jet reconstruction begins with seed calorimeter towers of size $\Delta\eta \times \Delta\phi = 0.1 \times 0.1$ with more than 1.0 GeV transverse energy. The transverse energies of towers in the cone around the seed tower are summed. The jet direction is then calculated using cell directions weighted by their transverse energies. The procedure is repeated until the jet axis converges. Two overlapping jets which share less than 50% of their total energy are kept as two separate jets. The shared energy is equally divided between the jets. Two overlapping jets are merged into a single jet if they share more than 50% energy. The jet energies have been calibrated using direct photon candidates by balancing jet p_T against that of the photon candidate.
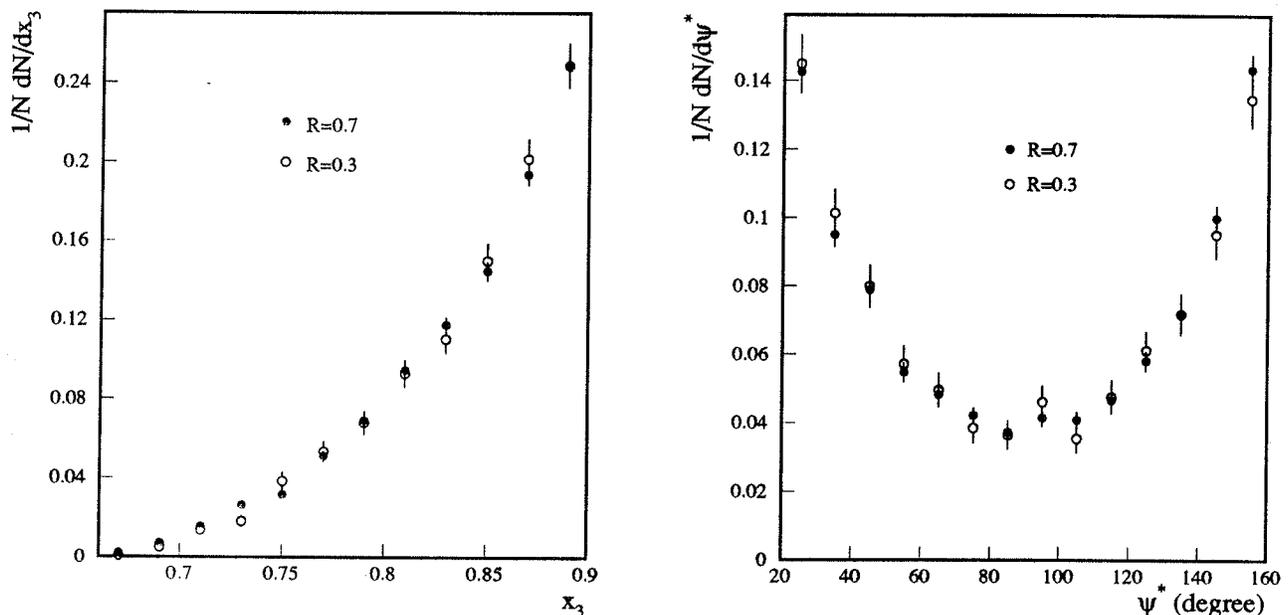

Figure 1: The (a) x_3 and (b) ψ^* distributions of the three-jet event samples selected by cone sizes of 0.7 (black dot) and 0.3 (circle) respectively. The distributions from two samples agree well within their statistical errors. It suggests that there is no significant bias in the topological distributions from the choice of jet cone size.

To select three- and four-jet events for topological studies, jets are required to have p_T greater than 20.0 and within η range of (-3.0, 3.0). In addition, the separation between jets in $\eta \times \phi$ space must be greater than 1.0. This requirement removes events with overlapped jets and therefore ensures good jet energy and direction measurements. To match the trigger requirement, there must be at least one jet in an event with p_T above 60.0 GeV. The surviving events with three (four) or more jets are classified as the three-jet (four-jet) events. The 60.GeV trigger-matching p_T cut in event selection enhances centrally produced events. To probe the structures of the three-jet and four-jet events over a large phase space, the events are further required to have an invariant mass of jet system greater than 250.0 GeV. This enhances relative contributions from forward and backward events.

5

For the three-jet analysis, x_3 is required to be less than 0.9 to ensure that the three jets are well separated in their center-of-mass system. Possible trigger bias in the forward regions due to the vertex displacement along the z-direction at the DØ interaction point is reduced by imposing two additional requirements: $\cos\theta^* < 0.95$ and $20° < \psi^* < 160°$. After all cuts, a sample of 7179 three-jet events remains.

Instead of making tight cuts to reduce possible selection bias, the four-jet events are analyzed without introducing additional cuts. This approach allows one to identify possible phase space regions which may distort topological distributions. There are 9008 events in the four-jet event sample.

The fourth jet, if any, in a three-jet event is ignored. Similarly, the fifth jet, if present, is not used in the four-jet analysis. To check the possible bias in the topological distributions from the choice of cone size in the jet reconstruction, the three-jet analysis is repeated using jets reconstructed with a cone size of 0.3. The measured x_3 and ψ^* distributions are compared with those of a cone size of 0.7 in figure 1. Distributions from two samples agree within their statistical errors. Evidently, the choice of different cone size does not change the distributions.
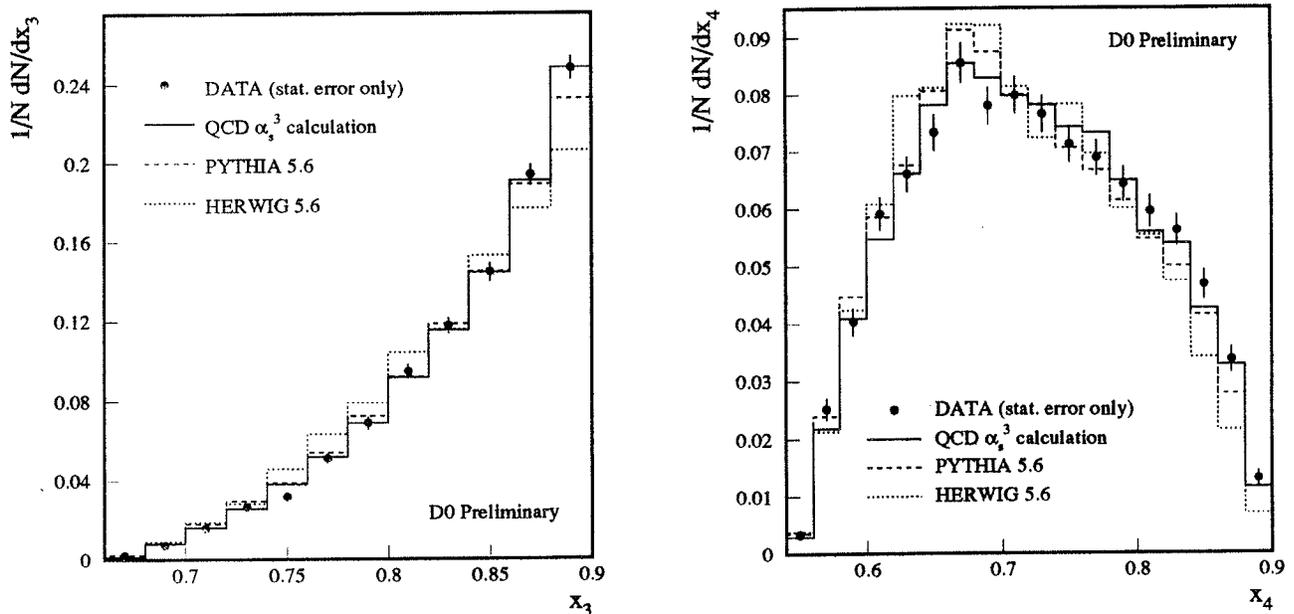

Figure 2: The scaled energy distribution of (a) the leading and (b) the next-to-leading jets of the three-jet events in their center-of-mass system. The QCD α_s^3 curve is the exact tree level calculation obtained from the PAPAGENO program. The peak toward high x_3 value is due to parton bremsstrahlung.

Comparison between Data and Predictions

The measured topological distributions for the three- and four-jet events are compared with predictions of QCD models. Distributions are normalized to unity. With a relatively large cone size in

the jet reconstruction, a high jet p_T cutoff, and a large separation between jets, the effects on the topological distributions due to soft bremsstrahlung and hadronization are expected to be small. In other words, the topological distributions should be insensitive to the jet internal structures. As results of hermetic, uniform and highly segmented DØ calorimeter, the uncertainties on the jet direction measurements are about 0.03 in η and 0.03 in ϕ, which are significantly small compared with the jet cone size and the separation between jets used in the event selection. The possible distortions in the topological distributions due to the uncertainty of energy scale should be small since only the energy fraction variables are relevant for the analysis. In addition, the measured distributions are weakly affected, if at all, by the inefficiencies of trigger, detector and event selection as a result of relative normalization. Consequently, the topological distributions of jets are expected to follow closely to those of their parent partons, as proposed by Local Parton-Hadron Duality (LPHD) [25]. This suggests that data distributions can be directly compared with the parton distributions of perturbative QCD calculations and with the particle distributions of Monte Carlo models. Nevertheless, the detector effects on the topological distributions are checked using fully simulated HERWIG events. Within the statistical uncertainty, the distributions determined from the calorimeter information agree with those determined from the particle level information.

In the following comparisons, the partonic event generator PAPAGENO [16] program was used to obtain the leading order QCD predictions with the QCD scale parameter set to 200 MeV. The exact tree level matrix elements calculation was employed for the three-jet analysis while the KS approximation [13] was used for the four-jet studies. The generated partons were analyzed as if they were observed jets and the selection criteria described above were applied to select three- and four-jet events. To obtain the predictions of PYTHIA 5.6 and HERWIG 5.6 Monte Carlo models, PYTHIA and HERWIG two-jet events with subsequent parton shower were generated using their default parameters apart from some kinematic cuts [2] to generate events more effectively. The partons were then fragmented to colorless hadrons with their respective hadronization models. Jets were reconstructed from the final state particles using the cone jet algorithm with a size of 0.7. The events are subjected to the same selection criteria as applied to the data. The topological variables for the surviving events were calculated from the reconstructed particle level jets. For all three programs, Duke-Owens set 1 [24] was used for the parton density function. It should be noted that PAPAGENO program generates exclusively three- or four-jet events and the inclusive three- or four-jet events are selected for the DATA and for the PYTHIA and HERWIG models. The topological distributions of exclusive event sample are compared with those of inclusive sample for the DATA and for the PYTHIA and HERWIG models, respectively. No significant differences in the two sets of distributions are observed.

The Topologies of the Three-Jet Events

Figure 2 shows the measured x_3 and x_4 distributions for the final three-jet events. The x_3 distribution peaks strongly as it approaches unity. It corresponds to a small x_5 value and reflects the dominance of soft quark and gluon bremsstrahlung. Also shown in the figure are the predictions of the leading order QCD calculation obtained from PAPAGENO, and the predictions of the PYTHIA and HERWIG Monte Carlo models. The leading order QCD calculation is in good agreement with the data. The main features of x_3 and x_4 distributions are also described by the HERWIG and PYTHIA models. However, the HERWIG prediction shows a deficit in both the x_3 and the x_4 distributions

---

[2]The modified PYTHIA parameters and their values are: MSEL=1, CKIN(1)=200.0 CKIN(3)=50.0 CKIN(27)=-0.99 and CKIN(28)=0.99. The modified HERWIG parameters and their values are: IPROC=1500, PTMIN=50.0 YJMIN=-4.0 and YJMAX=4.0

near $x = 1$.

The $\cos\theta^*$ distribution is shown in figure 3. Similar to the angular distribution of two-jet events, the characteristic angular dependence of Rutherford scattering is unmistakable. The large coverage of the DØ calorimeter allows the analysis to $\cos\theta^* = 0.95$. As evident in the figure, the data are well reproduced by the prediction of leading order QCD over a wide range of $\cos\theta^*$. Also evident is a surplus by HERWIG and a deficit by PYTHIA in the rate estimation at large values of $\cos\theta^*$.

The ψ^* distribution is a probe of initial state radiation. The measured ψ^* distribution is shown in figure 4 together with the results of the PAPAGENO, HERWIG and PYTHIA Monte Carlo programs. The enhancement due to the initial state radiation at $\psi^* = 20°$ and $\psi^* = 160°$ are clearly visible. As in the case of x_3, x_4 and $\cos\theta^*$ distributions, the agreement between data and the leading order QCD is excellent. However, both HERWIG and PYTHIA programs fail to correctly estimate the relative rates at different ψ^* values. Given the similarity in HERWIG and PYTHIA distributions and the small hadronization effect, the disagreement implies that the initial state radiation is not well accounted for by the parton shower programs investigated in this note.
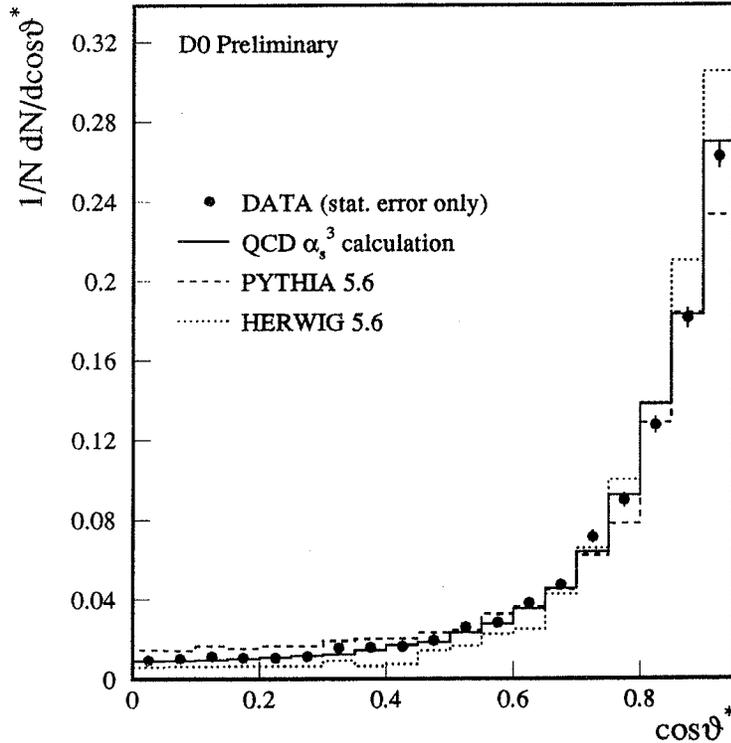

Figure 3: The distribution of the cosine of the leading jet polar angle of the three-jet events in their center-of-mass system. The peak at large $\cos\theta^*$ value is the result of the dominant t-channel exchange. The $\mathcal{O}(\alpha_s^3)$ QCD prediction is the exact tree level calculation obtained from the PAPAGENO program.

The energy asymmetry variable $\cos\delta$ for the three-jet events is compared with the leading order QCD calculation as well as the predictions with PYTHIA and HERWIG models in figure 5. The QCD calculation agrees with the data while HERWIG slightly overestimates the relative rate of symmetric
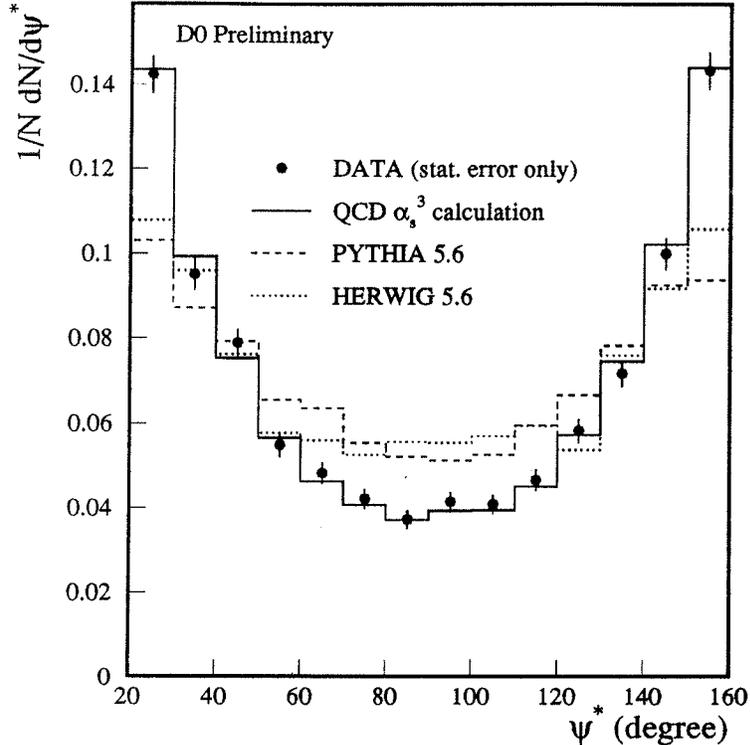
8

Figure 4: The distribution of the angle between the plane defined by the leading jet and beam line and the plane defined by the two non-leading jets of the three-jet events in their center-of-mass system. The enhancements at low and high ψ^* values are characteristics of initial state radiation. The $\mathcal{O}(\alpha_s^3)$ QCD prediction is the exact tree level calculation obtained from the PAPAGENO program.

events. In e^+e^- collisions, $\cos\delta$ distribution is a sensitive test of gluon spin. In fact, the data distribution shown here is very similar to that of the e^+e^- collisions [10].

The Topologies of the Four-Jet Events

The energy fractions carried by the two non-leading jets of the four-jet events are plotted in figure 6. The four jets are ordered in the order of decreasing energy in their center-of-mass system and labeled from 3 to 6. The predictions of the leading order QCD calculation and the parton shower Monte Carlo models are very similar and agree with the data in general.

The 4-jet $\cos\theta^*$ distribution (cosine of the leading jet polar angle of the four-jet events in their center-of-mass system) is compared in figure 7 with the leading order QCD calculation and the predictions from the PYTHIA and HERWIG models. Different from figure 3, the data are shown for the entire $\cos\theta^*$ range. The Monte Carlo models reproduce $\cos\theta^*$ distribution apart from the last $\cos\theta^*$ bin. The data in this bin are not reproduced by either the leading order QCD calculation nor the predictions of the parton shower Monte Carlo models. It is likely due to low acceptance at the boundary of η cut due to the displaced vertices. It should be noted that the PYTHIA prediction
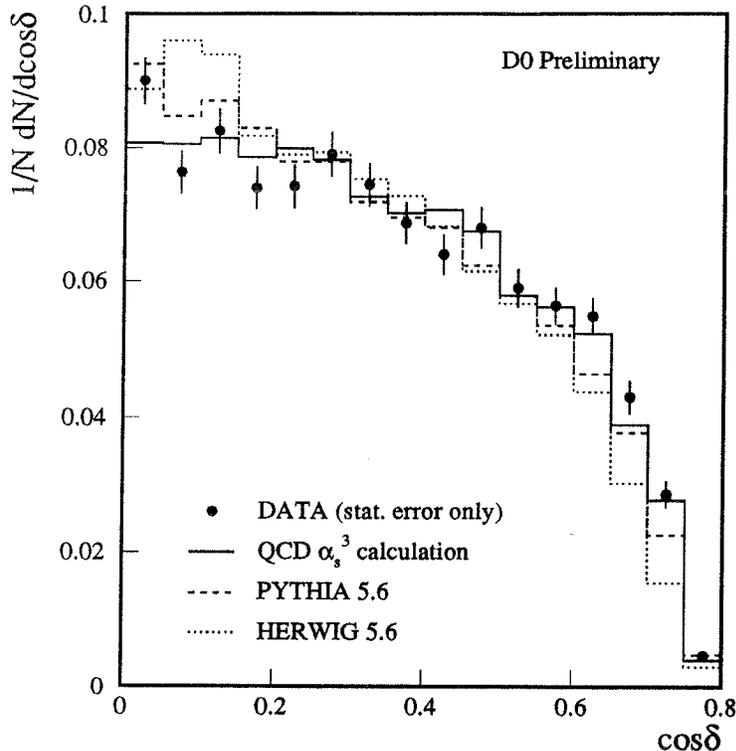
9

Figure 5: The distribution of the energy asymmetry variable between the two non-leading jets of the three-jet events in their center-of-mass system. The $\mathcal{O}(\alpha_s^3)$ QCD prediction is the exact tree level calculation obtained from the PAPAGENO program.

is significantly different from those of the KS [13] approximation and the HERWIG program in the forward region.

The distribution of the angle between the plane defined by the two leading jets and the plane defined by the two non-leading jets is shown in figure 8. The leading order QCD calculation and HERWIG program provide good descriptions of the data. The agreement between the data and the PYTHIA model is relatively poor in this case. The ψ^* distribution is sensitive to the gluon self-coupling and has been used to differentiate between QCD and QED-like models at e^+e^- collider [4]. It is worth while to note that the ψ^* distribution observed here is in many ways similar to that observed in the e^+e^- collisions.

Although no explicit cuts on topological variables are applied for the four-jet events, the leading order QCD calculations describe the data well. This is due to the fact that the phase space at which the truncated matrix element calculation diverges is essentially removed by high jet p_T cut and the large separation between the jets.

Figure 9 shows the angle distributions between all the possible jet pairs of the four-jet events in their center-of-mass system. For this study, the jets are ordered in decreasing order of p_T and labeled from 3 to 6. The distributions obtained from the PAPAGENO, PYTHIA and HERWIG Monte Carlo programs are also shown. In general, the trends of all six distributions are reasonably well described

10

by KS [13] approximation and the two parton shower Monte Carlo programs, in spite of disagreements in some regions of phase space.

In summary, the observed topological distributions of the three- and four-jet events produced in $\bar{p}p$ collision are consistent with the leading order QCD calculations. The PYTHIA and HERWIG models do not describe the data well. It should be noted that no attempt has been made to optimize generation parameters, for example the parton shower scale and cutoff parameters, of the PYTHIA and HERWIG models in order to obtain better agreement between the data and the predictions.
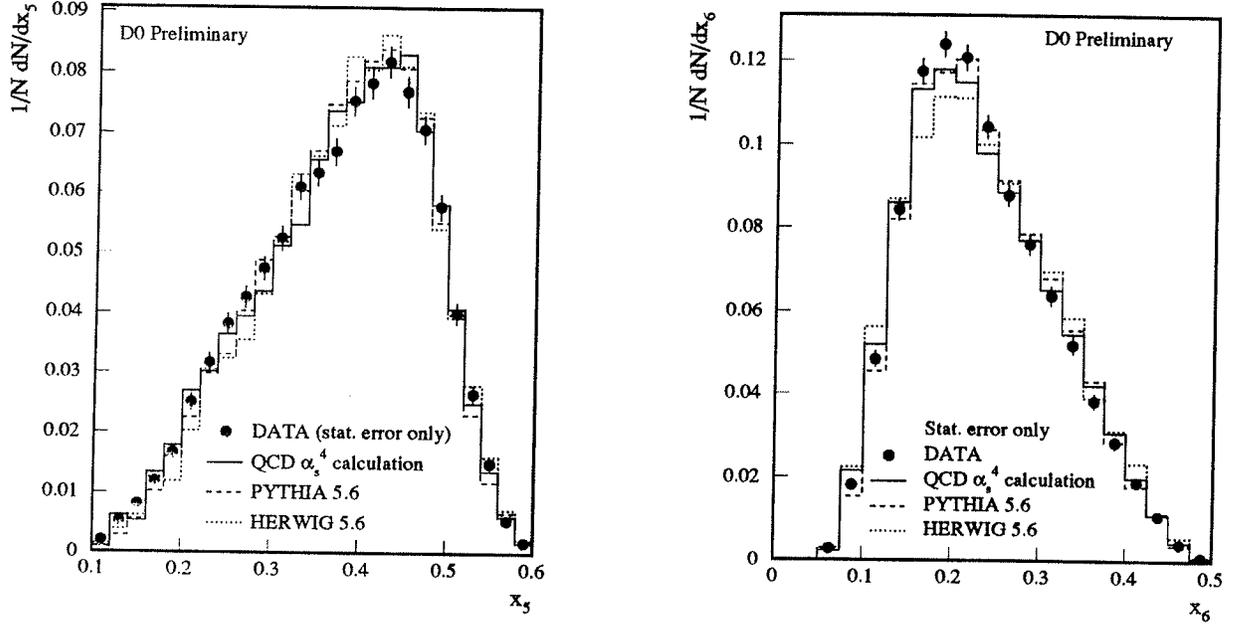

Figure 6: The energy fractions of the two non-leading jets of the four-jet events in their center-of-mass system. The jets are ordered in decreasing CMS energy and labeled from 3 to 6. The $\mathcal{O}(\alpha_s^4)$ prediction is the result of KS approximation obtained from the PAPAGENO program.

Summary

From a data sample of 15.5 pb^{-1} recorded by the DØ detector in $\bar{p}p$ collisions at $\sqrt{s} = 1800$ GeV at the Tevatron during the 1992-1993 running period, high statistics three-jet and four-jet event samples have been selected. A large number of distributions characterizing the global structures of the three- and four-jet events has been compared with the leading order QCD calculations and with the predictions of PYTHIA and HERWIG Monte Carlo models.

For the three-jet events, the investigated topological variables are: energy fractions carried by the two leading jets, the cosine of the leading jet polar angle, and the angle between the plane containing the leading jet and beam line and the plane containing the two non-leading jets. In the case of the four-jet events, the energy fractions carried by the two non-leading jets, the cosine of the leading jet

polar angle, the angle between the plane defined by the two leading jets and the plane defined by the other two non-leading jets as well as the six space angles between the jets have been studied.

Studies show that the observed topologies of the three- and four-jet events are well reproduced by the leading order QCD calculations. The PYTHIA and HERWIG Monte Carlo models do not provide a satisfactory description of the three- and four-jet events, specially in the very forward/backward phase space regions and for distributions sensitive to the initial state radiation.
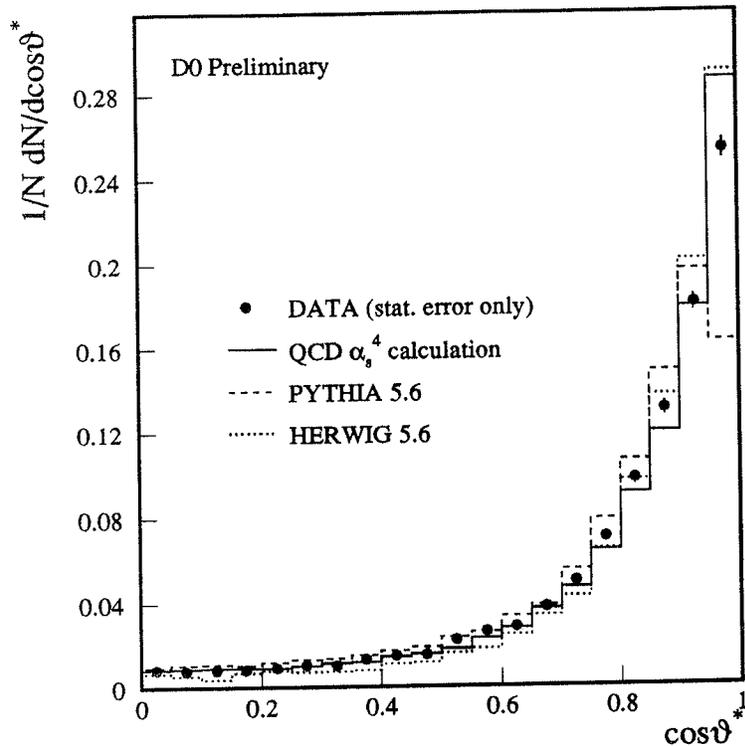

Figure 7: The distribution of the cosine of the leading jet polar angle of the four-jet events in their center-of-mass system. The $\mathcal{O}(\alpha_s^4)$ prediction is the result of KS approximation obtained from the PAPAGENO program.

References

[1] M. Gell-Mann, *Acta Physica Austriaca*, Suppl. **IX** (1972) 733;
    H. Fritzsch and M. Gell-Mann, 16th International Conference on High Energy Physics, Batavia, 1972; editors J.D. Jackson and A. Roberts, National Accelerator Laboratory (1972);
    H. Fritzsch, M. Gell-Mann and H. Leytwyler, **Phys. Lett. B47** (1973) 365.

[2] D.J. Gross and F. Wilczek, Phys. Rev. Lett. **30** (1973) 1343; Phys. Rev. **D8** (1973) 3633;
    H.D. Politzer, Phys. Rev. Lett. **30** (1973) 1346;
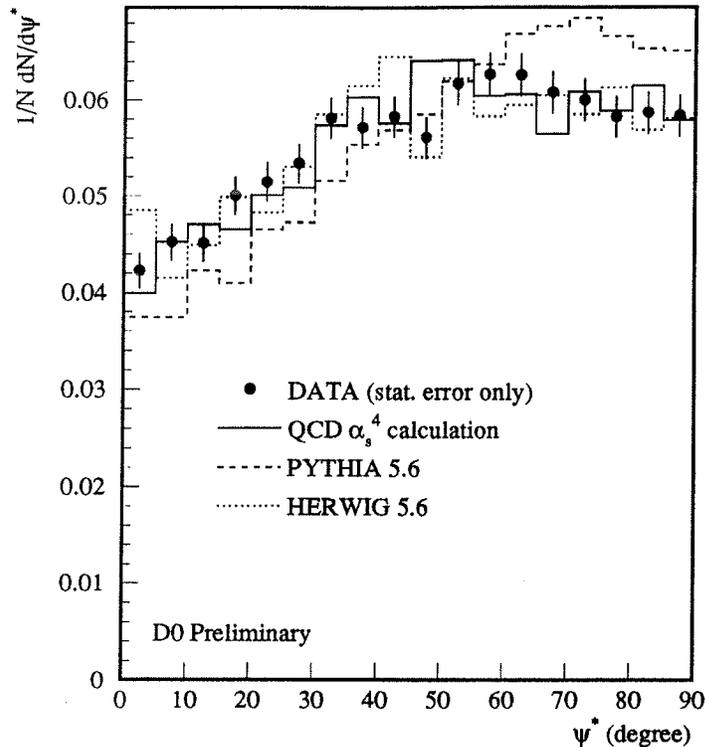
[3] G. 't Hofft, Nucl. Phys. **B33** (1971) 173.

Figure 8: The distribution of the angle between the plane containing the two leading jets and the plane containing the other two non-leading jets of the four-jet events in their center-of-mass system. The $\mathcal{O}(\alpha_s^4)$ prediction is the result of KS approximation obtained from the PAPAGENO program.

[4] For recent reviews on QCD test at e^+e^- collider see:
S. Bethke, J.E. Pilcher, *Annu. Rev. Nucl. Part. Sci.*, **42** (1992) 251;
T. Hebbeker, Phys. Rep. **217** (1992) 69.

[5] For recent reviews on QCD test at $\bar{p}p$ collider see:
J.E. Huth and M.L. Mangano, "QCD Tests in Proton-Antiproton Collisions" Fermilab preprint Fermilab-Pub-93/019-E (1993);
R.K. Ellis and W.J. Stirling, "QCD and Collider Physics", Fermilab preprint Fermilab-Conf-90/164-T (1990).

[6] DØ Collaboration, S. Abachi *et al.*, "Jet Cross Sections and Angular Distributions at Dzero", DØ note #1829.

[7] UA1 Collaboration, G. Arnison *et al.*, Phys. Lett. **B158** (1985) 494;
UA2 Collaboration, J.A. Appel *et al.*, Z. Phys. **C30** (1986) 341;
CDF Collaboration, F. Abe *et al.*, Phys. Rev. **D45** (1992) 1448.

[8] UA2 Collaboration, J. Alitti *et al.*, Phys. Lett. **B268** (1991) 145.

[9] CDF Collaboration, F. Abe *et al.*, Fermilab Preprint Fermilab-Pub-93/003-E (1993).

[10] TASSO Collaboration, R. Brandelik *et al.*, Phys. Lett. **B97** (1980) 453;
PLUTO Collaboration, C. Berger *et al.*, Phys. Lett. **B97** (1980) 459;
CELLO Collaboration, H.J. Behrend *et al.*, Phys. Lett. **B110** (1982) 329;
R. Clare (MARK-J Collaboration), "QCD Properties of Jets", MIT Ph.D. Thesis (1982);
S.L. Wu, Phys. Rep. **107** (1984) 59.

[11] Z. Kunszt and E. Pietarinen, Nucl. Phys. **B164** (1980) 45;
T. Gottschal and D. Sivers, Phys. Rev. **D21** (1980) 102;
F.A. Berends *et al.*, Phys. Lett., **B118** (1981) 124.

[12] F.A. Berends, W.T. Giele and H. Kuijf, Nucl. Phys. **B333** (1990) 120; Phys. Lett. **B232** (1990) 266.

[13] Z. Kunszt and W.J. Stirling, Phys. Lett. **B171** (1986) 307; Phys. Rev. **D56** (1988) 2439.

[14] C.J. Maxwell, Phys. Lett. **B192** (1987) 190; Nucl. Phys. **B316** (1989) 321;
M.L. Mangano and S.J. Parke, Phys. Rev. **D39** (1989) 758;
C.J. Maxwell and S.J. Parke, Phys. Rev. **D44** (1991) 2727.

[15] K. Konishi, A. Ukawa, and G. Veneziano, Nucl. Phys. **B157** (1979) 45;
R. Odorico, Nucl. Phys. **B172** (1980) 157;
G.C. Fox and S. Wolfram, Nucl. Phys. **B168** (1980) 285;
T.D. Gottschalk, Nucl. Phys. **B214** (1983) 201;
G. Marchesini and B.R. Webber, Nucl. Phys. **B238** (1984) 1;
B.R. Webber, Nucl. Phys. **B238** (1984) 492.

[16] I. Hinchliffe, "PAPAGENO - Partonic Event Generator V 3.60", private communication.

[17] PYTHIA 5.6 Program:
H.U. Bengtsson and T. Sjöstrand, Comp. Phys. Comm. **46** (1987) 43.

[18] HERWIG 5.6 Program:
G. Marchesini and B. Webber, Nucl. Phys. **B310** (1988) 461;
I.G. Knowles, Nucl. Phys. **B310** (1988) 571;
G. Marchesini *et al.*, Comp. Phys. Comm. **67** (1992) 465.

[19] X. Artru and G. Mennessier, Nucl. Phys. **B70** (1974) 93;
B. Andersson, G. Gustafson, and T. Sjöstrand, Z. Phys. **C6** (1980) 235;
B. Andersson *et al.*, Phys. Rep. **97** (1983) 31.

[20] R.D. Field and S. Wolfram, Nucl. Phys. **B213** (1983) 65.

[21] S. Abachi *et al.*, "The Dzero Detector" Fermilab Preprint Fermilab-Pub-93/179 (1993).

[22] J. Linnemann, "The DØ Trigger" in Proceedings of the 7th Meeting of the APS Division of Particles and Fields, Batavia (1992);
R. Astur and A. Milder, "Jet Trigger Efficiency in the DØ Detector", DØ note #1663.

[23] UA1 Collaboration, G. Arnison *et al.*, Phys. Lett. **B132** (1983) 214.

[24] D.W. Duke and J.F. Owens, Phys. Rev. **D30** (1984) 49;
J.F. Owens, Phys. Lett. **B266** (1991) 126.

[25] Y.I. Azimov *et al.*, Z. Phys. **C27** (1985) 65;
Yu.L. Dokshitzer, V.A. Khoze and S.I. Troyan, "Perturbative QCD", Singapore: World Scientific (1989) 241;
D. Amati and G. Veneziano, Phys. Lett. **B83** (1979) 87;
G. Marchesini, L. Trentadue and G. Veneziano, Nucl. Phys. **B181** (1981) 335.
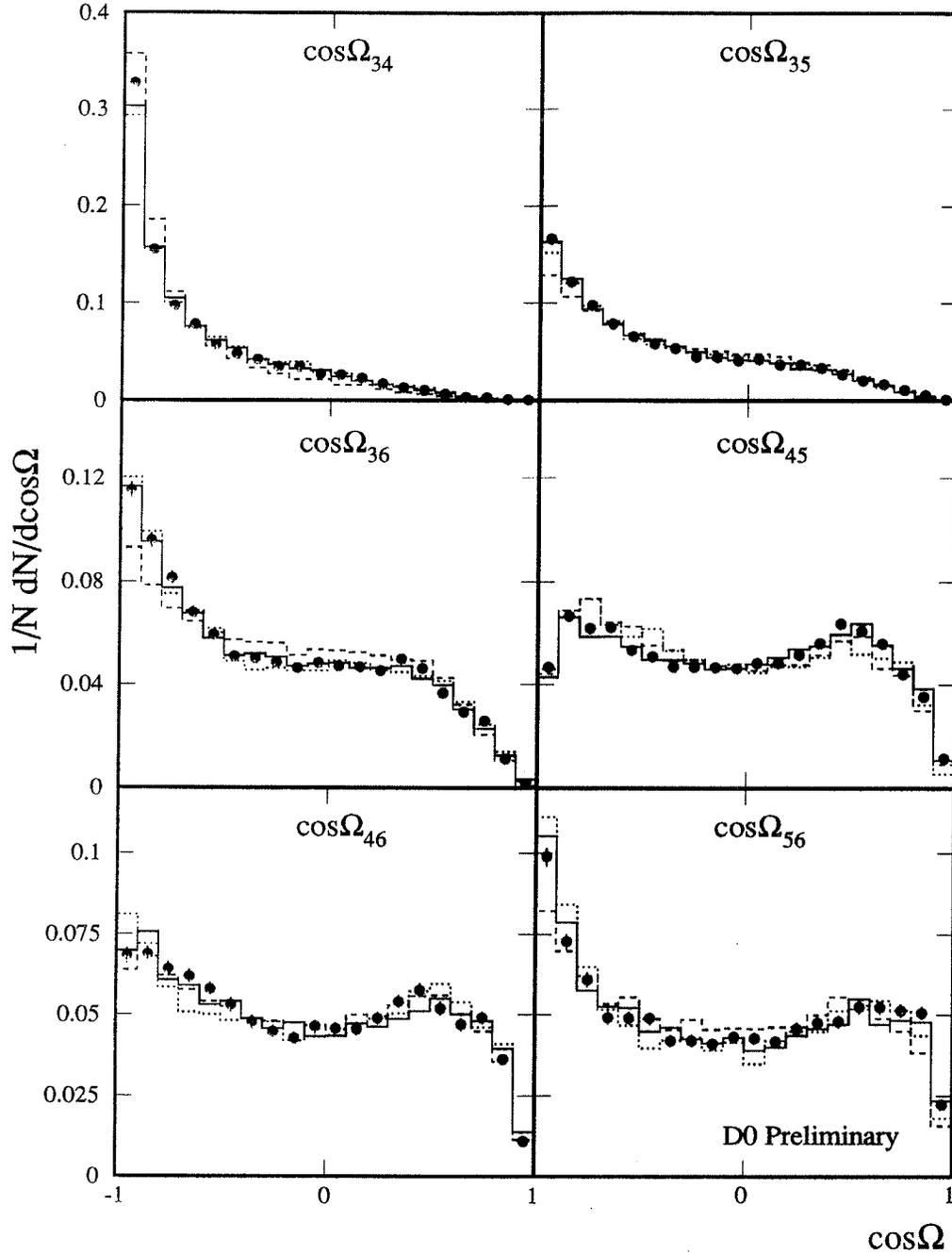
Figure 9: Cosines of space angles between all jets in their center-of-mass system for the four-jet events. The jets are ordered from 3 to 6 in descending p_T. The predictions of the leading order QCD, the PYTHIA and HERWIG Monte Carlo models are plotted as solid, dash and dot lines respectively. The leading order QCD curve is the result of KS approximation obtained from the PAPAGENO program.